-RESEARCH PAPER-

International Journal of Mining and Geo-Engineering IJMGE

IJMGE 56-3 (2022) 239-247 DOI: 10.22059/IJMGE.2022.329665.594927

Removal of copper ions from dilute sulfuric acid solutions: Effect of solution composition and applied potential

Saeed Hassani Sadrabadi[a], Hojat Naderi[a, *], Hamid Reza Zare [b], Seyed Mohammad Moshtaghioun [c]

[a] *Mining & Metallurgical Engineering Department, Yazd University, Yazd, Iran.*
[b] *Department of Chemistry, Yazd University, Yazd, Iran.*
[c] *Department of Biology, Yazd University, Yazd, Iran.*

Article History:
Received: 28 August 2021.
Revised: 06 December 2021.
Accepted: 04 March 2022.

ABSTRACT

Removal of copper from synthesized and real dilute sulfuric acid solutions was investigated. Effects of copper, iron concentrations and applied potential were studied. In pure copper solutions, increasing the Cu^{2+} concentration from 1000 to 5000 mg.L^{-1} increased the copper recovery from about 30-300% depending on the cathode potential and decreased the energy consumption by about 30%. Also, increasing the acid concentration from 15 to 50 g.L^{-1} and about a 25% increase in copper recovery and a 30% decrease in energy consumption were observed. The addition of Fe^{2+} to the solution improved the ionic conductivity and so that the copper recovery. The specified energy consumption for the real leaching solutions increased to 31-47 KWh.kg^{-1}. The diffusion coefficients for several synthesized and real copper electrowinning electrolytes were determined. Moreover, the maximum value of the diffusion coefficient (D) was obtained 2.27*10^{-4} cm^2.s^{-1} for the pure copper solution at a concentration of 1000 mg.L^{-1} Cu^{2+} which was higher than impure and real solutions.

Keywords: *Chronoamperometry, Copper, Cyclic voltammetry, Dilute solution, Electrodeposition, Diffusion Coefficient.*

1. Introduction

Heap leaching is favored today for the extraction of copper from low-grade ores because of the simplicity of design, shorter startup times, and larger volumes being processed at low capital and operating costs [1]. However, processing of a huge amount of low-grade ore causes serious problems such as lower copper-cathode-production efficiency from such a low-concentrated pregnant leach solution (PLS) in the solvent extraction and electrowinning (SX-EW) plants [2]. The PLS usually contains up to ca. 2 g.L^{-1} of copper, while the iron concentration is up to ca. 5 g.L^{-1} due to e.g. leaching of iron minerals [3]. Also, it contains an extensive area of elements, such as Cu, Fe, Ni, Zn, etc.

Electrochemical technology is a helpful method for the removal or recovery of metals from solutions [4]. In addition, electrochemical processes offer a minimum generation of solid waste, simultaneously reducing the processing cost for solid waste disposal. As such, electrochemical technologies can potentially suggest the best solution for the treatment of dilute solutions such as wastewaters [4, 5].

The wastewater treatments containing Cu have been carried out by various techniques, such as chemical precipitation [6], coagulating sedimentation [7], adsorption [8], ion exchange, membrane separation [9], electrochemical methods [10], and novel technologies such as microbial fuel cells (MFCs) [11, 12]. In 2020, Xueyi Guo et al. performed the hydrolysis precipitation and cyclone electrowinning to recover the Sn and Cu in the solutions. With these techniques, 92.75% Sn was precipitated and the smooth cathode copper (purity 99.98%) was obtained with the current efficiency was 94.96% [13]. Jose Angel Barragan et al. used an electrochemical reactor with a rotating cylinder electrode (RCE) to evaluate the copper concentration decrement, the cathodic current efficiency, the specific energy consumption, and mass transfer coefficient [14]. Also, some researchers investigated the recovery of copper from solutions by electrowinning on glassy carbon and carbon nanotube film [15].

Nearly 20% of annual Cu production is carried out using electrowinning (EW) [16]. industrial electrowinning, the typical operating conditions are cell voltage of ca. 2 V, copper ion concentration of ca. 50 g.L^{-1}, current density of 20-45 mA.cm^{-2}, temperature of 40-60° C, current efficiency of 89-94% and specific energy consumption of 1.8-2.5 kWh.kg^{-1} of copper. [17]. Higher copper concentrations decrease mass transfer limitations resulting in higher current efficiency [18]. Since high current density within electrowinning moreover increases the ohmic resistance losses in the solution, small operational current densities tend to correlate with low power consumption [19, 20]. The theoretical minimum energy consumption of industrial copper electrowinning is 0.75 kWh.kg^{-1} Cu when no efficiency losses occur [17].

The application of EW for dilute leaching solutions purification, specifically the removal of Cu, is indeed a difficult approach since the recovery of metals from dilute solutions is known to involve high operating expenses. Therefore, to make optimal use of mining solutions, studying the parameters involved in the extraction of copper from leaching solutions is necessary. So, an effort to decline the energy consumption of electrowinning from dilute solutions would increase its viability as a stable recovery procedure for acidic metal-containing solutions.

In this study, the electrodeposition of copper from synthesized and real dilute leaching solutions was studied. Effects of solution composition and cathode potential on copper recovery, impurities co-deposition, and specific energy consumption were investigated.

---

* Corresponding author. Tel/Fax: +98 3538210995, *E-mail address:* naderi@yazd.ac.ir (H. Naderi).

2. Materials and Methods

2.1. Materials

Copper (II) sulfate, iron (II) sulfate, sulfuric and nitric acids in the analytical grade were provided from Merck Company, Germany. Synthesized solutions were prepared using deionized water and the addition of the desired concentrations of chemicals and pHs. Real leaching solutions originated from the Kaveh copper heap leaching plant, Yazd, Iran. Table 1 shows the real leaching solution compositions and characteristics.

2.2. Equipment

Cyclic voltammetry (CV) and chronoamperometry (CA) tests were performed in a typical three-electrode cell controlled by a potentiostat-galvanostat device (Sama Researcher Center, SAMA 500 Model, Iran). Saturated calomel electrode (SCE, 0.244 V vs. SHE, Metrohm Co., Switzerland) and a platinum electrode (99.95%, Azar Electrode Co., Iran) were used as the reference and counter electrodes, respectively, while the working electrode was a titanium plate (99.95%, Azar Electrode Co., Iran) with a surface area of 14 cm^2. During the experiments, the cell voltage was measured by a digital multimeter (Marmonix Co., TS97 Model, Canada) which was connected between the counter and working electrodes. Solution pH was measured using a Metrohm pH meter (Metrohm Co., Model 827, Switzerland). The electrochemical cell was operated for copper recovery and related experiments as shown in Figure 1.

2.3. Experiments

Firstly, the electrochemical cell preparation was done. 150 mL of the (synthesized or real) solution was poured. Reference, counter, and well-polished working electrodes were inserted in the cell. The distance between working and counter electrodes was kept constant at 3.0 ± 0.1 cm. All measurements were performed at room temperature (T=26° C ± 1) for 2 hours. Cyclic voltammetry tests were performed using an H_2SO_4 solution (pH 2) in the potential range of -0.8 to +0.8 V vs. SCE with the scan rate of 10 mV.S^{-1}. The effect of Cu (II) (1000, 2000, and 3000 mg.L^{-1}) and Fe (II) (1000, 3000, and 5000 mg.L^{-1}) concentrations on the copper reduction potential were investigated. Based on the results obtained from CV tests, chronoamperometry experiments were carried out at the potentials of -0.1, -0.2 and, -0.3 V vs. SCE, and the effect of parameters such as H_2SO_4 concentration (0, 15, 30. and 50 g.L^{-1}), Cu (II) concentration (1000, 3000 and 5000 mg.L^{-1}) and Fe (II) concentration (0, 2000, and 5000 mg.L^{-1}) on the copper electrodeposition was evaluated for 2 hours. Chronoamperometry experiments were repeated using the three real leaching solutions.

Table 1. Chemical analysis and characteristics of the studied real leaching solutions (concentrations of metals in mg.L^{-1}).

Solution code	pH	Conductivity (mS.cm^{-1})	Cu	Al	As	Ca	Cd	Ce	Co	Cr
R-S1	1.87	12.37	1109.00	275.00	1.50	396.00	0.20	0.39	3.48	0.37
R-S2	1.82	13.85	1114.00	334.00	1.47	406.00	0.22	0.48	3.84	0.41
R-S3	1.50	18.04	1022.00	260.00	1.04	402.00	0.19	0.39	2.99	0.30

Table 1. (Continued).

Solution code	Fe	K	Li	Mg	Mn	Na	Ni	Si	Ti	V	Zn
R-S1	1190.00	10.50	0.97	669.00	161.00	114.00	0.78	110.00	0.23	0.54	20.40
R-S2	1550.00	7.10	1.00	792.00	194.00	96.40	0.76	124.00	0.09	0.74	23.00
R-S3	1104.00	10.90	0.72	623.00	144.00	109.00	0.63	122.00	0.16	0.49	17.80

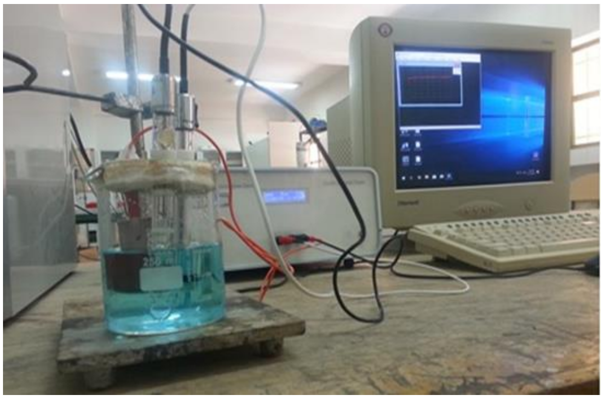

Figure 1. Experimental setup of the electrochemical cell.

2.4. Analytical Procedures and Electrochemical Measurements

After running the experiments, to quantify the amount of Cu and Fe sedimented on the working electrode, the working electrode samples were placed in 25 ml of 20% $\frac{V}{V}$ HNO_3 solution for 12 h to dissolve all of the deposits. Afterward, the Cu (II) concentration was determined by using an Atomic Absorption Spectrometer (Young Lin AAS-8000 Series, 8020 Model, Korea). The chemical analysis of the real leaching solutions was carried out using inductively coupled plasma mass spectrometry (Hewlett-Packard-HP 4500 ICP-MS, Agilent Technologies Inc., USA).

The cell voltage (V) consists of electrode potentials of anodic and cathodic reactions and from the I.R drop, as:

$$E_{Cell} = (E_C + |\eta_C|) - (E_A + |\eta_A|) - I.\, R_{Total} \quad (1)$$

Where E_C is the electrode potential of cathodic reaction, η_C is the cathodic reaction overpotential, E_A is the electrode potential of anodic reaction, η_A is the anodic reaction overpotential, I is the current passing through the electrochemical cell and R_{Total} is the total resistance of the electrochemical cell. The specific energy consumption (kWh.kg^{-1}) for the recovery of copper from the real leaching solutions on the titanium plate and the current efficiency (%) was calculated by equations 2 to 4, respectively:

$$\text{Specific Energy Consumption (SCE)} = \frac{ZFE_{Cell}}{\eta M.3600} \quad (2)$$

$$\text{Current Efficiency (CE)} = \left(\frac{m'}{m}\right) * 100 \quad (3)$$

$$m = \left(\frac{MIt}{ZF}\right) \quad (4)$$

Where Z is the number of electrons (=2), F is the Faraday constant (96,485 C.mol-1 e-), E_{cell} is the cell voltage observed during the experiments (V), η is the current efficiency, M is the molar mass of copper (63.546 g.mol-1), I is the current (A), t is the time (S), m/ is the amount of sediment obtained in practice (g) and m is the amount of theoretical sediment obtained according to the Faraday's law (g) [21]. The copper removal efficiency was calculated as:

$$RE_{Cu} = \frac{C_0 - C_t}{C_0} * 100\% \quad (5)$$

In equation 5, C_0 is the primary Cu (II) concentration fed into the electrochemical cell ($mg.L^{-1}$) and C_t is the residual Cu (II) concentration at duration t ($mg.L^{-1}$).

3. Results and discussion

3.1. Cyclic Voltammetry Results

3.1.2. Effect of Copper Concentration

Figure 2 shows the effect of copper concentrations on the cyclic voltammetry diagrams. The CV graphs consist of one cathodic and one anodic peak which their intensities linearly increase with the increasing of Cu (II) concentration. This behavior may be due to the presence of a large number of electroactive species at higher concentrations. The system also follows a diffusion-controlled mechanism [22].

There is no change in the number and location of the peaks. In the forward scan, an anodic peak (i_{pa}) at a potential of about +0.20 V vs. SCE, and in the reverse scan, a cathodic peak (i_{pc}) at a potential of about -0.20 V vs. SCE were observed. In the sequential redox couple of Cu (II)/Cu (0), the cathodic peak (i_{pc}) and the anodic peak (i_{pa}) correspond to the reduction of Cu (II) to Cu (0) and the oxidation of Cu (0) to Cu (II), respectively. The above result suggests that at pH 2, Cu (II) sustains a one-step two-electron transfer electrochemical redox reaction. The feasible mechanism of the redox reaction for the above cyclic voltammogram is as follow:

Cu (II) + $2e^-$ = Cu (0) (Reduction reaction) (6)

Cu (0) = Cu (II) + $2e^-$ (Oxidation reaction) (7)

Increasing the copper concentration causes an increase in the ionic strength of the solution and therefore changes the activity of the ions. As a result, the oxidation-reduction changes according to the Nernst equation and shifts the location of the peaks towards more positive values. The electrical potential of a metal (E_M^+) with its ion concentration ($[M^+]$) in solution is as follows [23]:

$$E_{M^+} = E^0_+ + \frac{0.059}{Z}\log\,[M^+] \tag{8}$$

Regarding the above equation, it is clear that the electrical potential of a metal decreases as the concentration of its ions decreases. Z is the number of electrons that participate in the reaction. In this formula, E_M^+ is the potential of the standard metal electrode obtained from the table of standard electrode potentials [23].

The peak current for both the anodic and cathodic peaks follows the equation [24]:

$$i_p = 2.69\times10^5\times n^{3/2}\times A\times D^{1/2}\times C\times v^{1/2} \tag{9}$$

Where, i_p = peak current in ampere (A), n = number of exchanged electrons, A = surface area of the electrode in cm^2, D = diffusion coefficient in cm^2/s, C = concentration of the species in mol/cm^3, v = scan rate in volts/s.

3.1.2. Effect of Fe (II) Presence and Concentration

Figure 3 shows the effect of Fe (II) concentration on the cyclic voltammetry diagrams. The results show that there is no change in the number of peaks, but it has changed the intensity of the peaks and has shifted the location of the peaks in small quantities towards more positive values. The addition of Fe (II) ions to the solution increases the solution ionic strength so that the activity of the ions changes. As a result, based on the Nernst equation, the solution potential changes.

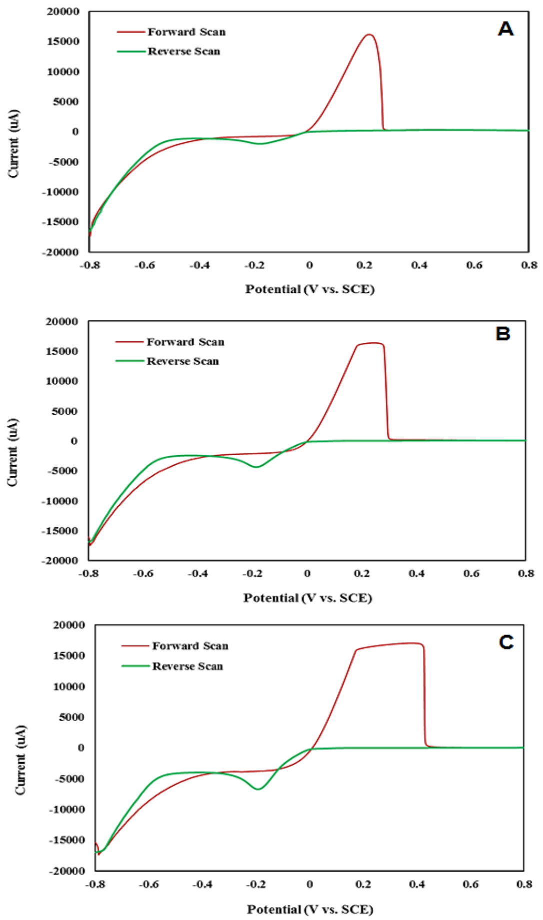

Figure 2. Cyclic voltammetry diagrams of a solution containing A) 1000, B) 2000 and, C) 3000 $mg.L^{-1}$ of Cu (II) (T=26° C ± 1, pH = 2, scan rate = 10 mVs^{-1}).

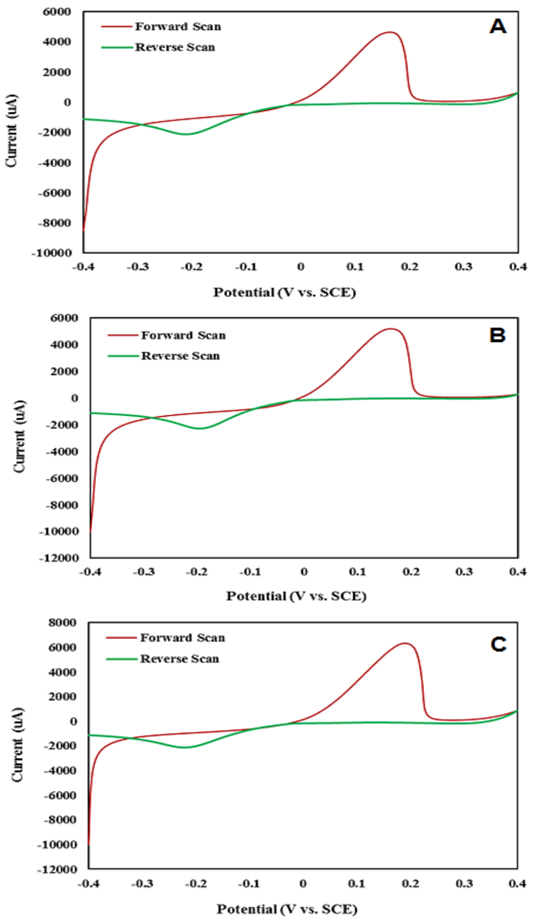

Figure 3. Cyclic voltammetry diagrams of a solution containing 1000 $mg.L^{-1}$ of Cu (II) and, A) 1000, B) 3000 and, C) 5000 $mg.L^{-1}$ of Fe (II) (T=26° C ± 1, pH = 2, scan rate = 10 mVs^{-1}).

3.2. Copper Electrodeposition by Chronoamperometry Technique

3.2.1. Effect of Copper Concentration and the Electrode Potential

Figure 4 shows the effect of initial copper concentration on the copper electrodeposition at different potentials. According to the results, increasing both Cu (II) concentration and potential has a positive effect on copper recovery.

Current density variations and the cell performance calculations are shown in Figure 5 and Table 2. Maximum removal percentage of 13% obtained at -0.3 V and 5000 mg.L^{-1} of Cu (II), at a current density of 18571 mA.m^{-2}, current efficiency of about 100% and, specific energy consumption of 1.71 kWh.kg^{-1}.

The description for this can be that enhancing the Cu (II) ion concentration in the electrolyte solution will feed an adequate and steady value of Cu (II) to the cathode surface, which improves the rate of deposition and consequently the efficiency as well as alternative parameters. Another effect of high Cu (II) concentration is the lower concentration polarization and the accompanying decrease of H_2 overvoltage [25]. Also, increasing the copper concentration slightly increases the diffusivity of cupric ions although at higher concentrations, the diffusion coefficient of cupric ions decreases [26].

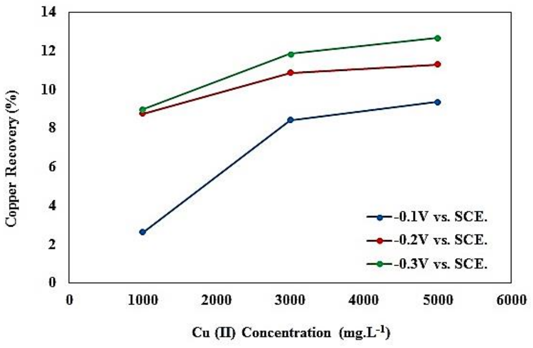

Figure 4. The effect of Cu (II) concentration and cathode potential on the copper electrodeposition (T = 26° C ± 1, pH = 2).

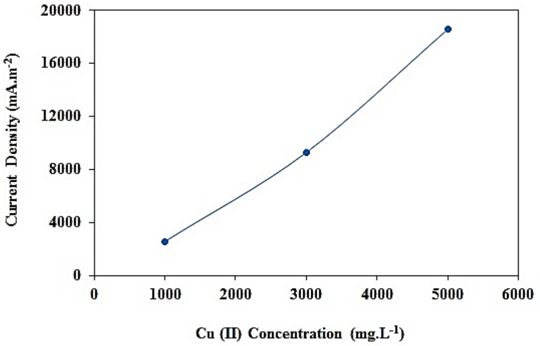

Figure 5. The effect of Cu (II) concentration on the current density at the potential of -0.3 V vs. SCE (T = 26° C ± 1, pH = 2).

3.2.2. Effect of Acid Concentration on the Electrochemical Cell Performance

The effect of H_2SO_4 concentration on the copper recovery was studied at -0.1 V vs. SCE. Figure 6 and Table 3 show the results.

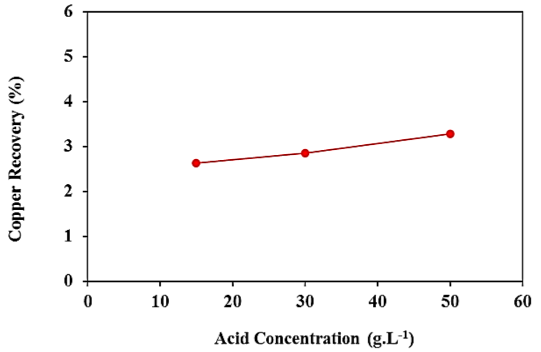

Figure 6. The effect of H_2SO_4 concentration on the copper electrodeposition at the potential of 0.1 V vs. SCE (T = 26° C ±1, [Cu (II)]=1000 mg.L^{-1}).

Table 2. The effect of Cu (II) concentration on the cell performance (T = 26° C ± 1, pH = 2).

Copper concentration (mg.L^{-1})	Time (S)	Cathode potential (V)	Average cell voltage (V)	Copper recovery (%)	Cathodic current efficiency (%)	Specific energy consumption (KWh.kg^{-1})
1000	7200	-0.3	2.72	8.98	93.78	2.45
3000	7200	-0.3	2.37	11.85	97.23	2.06
5000	7200	-0.3	2.13	12.67	100	1.71

Table 3. The effect of H_2SO_4 concentration on the cell performance at potential of -0.1 V vs. SCE (T = 26° C ± 1, [Cu (II)] = 1000 mg.L^{-1}).

H_2SO_4 concentration (g.L^{-1})	Time (S)	Average cell voltage (V)	Copper recovery (%)	Cathodic current efficiency (%)	Specific energy consumption (KWh.kg^{-1})
15	7200	2.63	2.64	72.76	2.96
30	7200	1.94	2.85	75.61	2.70
50	7200	1.70	3.28	78.44	2.01

As could be seen in Table 3, the increase of H_2SO_4 concentration in the electrolyte had a positive effect on the cell performance. Increasing acid concentration from 15 to 50 g.L^{-1} increased the cathodic current efficiency by about 6% and the copper recovery by about 1%. At the same time, cell voltage and specific energy consumption were decreased from 2.63 to 1.70 V and 2.96 to 2.01 KWh.kg^{-1}, respectively. This can be owing to improved electrolyte conductivity and therefore polarization of electrolyte, simultaneously with the improved dissolution of Cu (II) ions in the electrolyte. The principal disadvantage of increasing H_2SO_4 concentration in the electrolyte is the enhancement of viscosity and consequent decrement of diffusion of ions to the cathode surface. The results obtained by Moats et al. demonstrated that at an equivalent copper concentration, increasing the sulfuric acid concentration from 160 to 200 g.L^{-1} could decrease the diffusivity of the cupric ions by about 20% [26]. Therefore, acid concentration plays a significant role in the electrodeposition processes. This is due to the change in the difference between the electrode potentials of the solid and liquid phases when the electrolyte conductivity is increased. A problem is that a higher acid concentration can favor zones of metal dissolution within the three-dimensional electrode. To avoid or minimize metal dissolution, simultaneous consideration of the influences of acid concentration and current density is required. Very high acid concentrations in an electrowinning cell are not ever positive because the copper can be re-dissolved into the electrolyte after it has been plated at very high concentrations of acid.

3.2.3. Effect of Iron Concentration on the Electrochemical Cell Performance

The effect of iron in copper electrowinning solution in the hydrometallurgical process of SX-EW is well known. When the iron concentration in copper electrowinning solution increases, the current efficiency decreases, and energy consumption increases. Also, the surface morphology of the cathode changes. These effects intensify by increasing the flow rate of the solution [18]. The decrease in current efficiency and the increase in energy consumption is due to iron ions being oxidized from ferrous to ferric at the anode and conversely reduced from ferric to ferrous at the cathode [27]. Figure 7 shows the effect of Fe (II) concentration on the copper electrodeposition and iron recovered to the cathode as an impurity.

According to Figure 7, the presence of Fe (II) in the solution increases the copper recovery. Copper depositions of 2.64%, 3.65%, and, 5.09% were obtained in the presence of 0, 2000 and 5000 mg.L^{-1} of ferrous ions, respectively, although caused some iron impurities to enter in copper deposits.

This increase in copper sedimentation can be related to a decrease in the internal resistance of the system. The addition of Fe (II) improves the ionic conductivity of the solution. Increasing the Fe (II) concentrations from 2000 and 5000 mg.L^{-1} resulted in an increase in the current density from 929 to 1641 mA.m^{-2} and the solution conductivity from 14.87 to 19.35 mS.cm^{-1}. Figure 8 shows the chronoamperometry of copper electrowinning from synthetic solutions in concentrations of 2000 and 5000 mg.L^{-1} Fe^{2+} and pure solution.

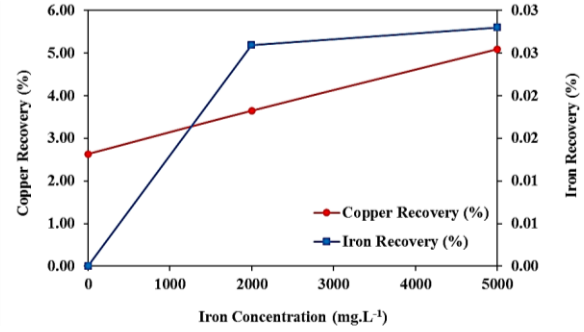

Figure 7. The effect of Fe (II) concentrations on the copper electrodeposition and iron recovered to the cathode at potential of -0.1 V vs. SCE (T = 26° C ± 1, pH = 2, [Cu (II)] = 1000 mg.L^{-1}).

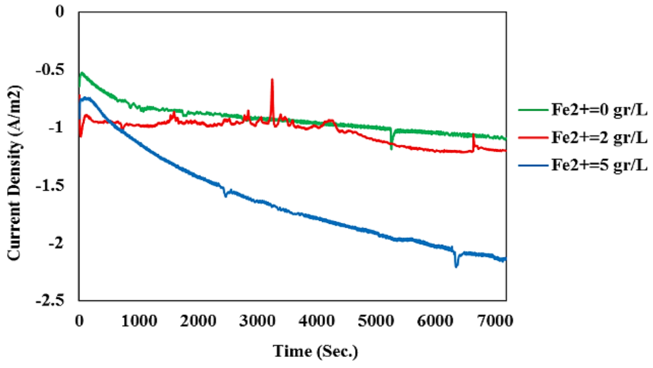

Figure 8. Chronoamperograms of copper electrowinning from synthetic solutions ($CuSO_4$ solution, Cu^{2+}=1000 mg.L^{-1}, pH=2, 2 hours and -0.1 V vs. SCE).

The manner of iron within electrowinning of copper from sulfate electrolytes is important, and its impact on the performance of the copper electrowinning process has been stated by [19] who have investigated the interaction of iron [Fe (II), Fe (III)] during copper electrowinning from dilute solutions, and [28] who have studied the mass transfer kinetics of the ferrous-ferric system in copper sulfate electrolyte. Iron is an important parameter affecting the systems of electrical copper recovery. It is well known that ferrous is a strong transition metal catalyst, which is applied in the electrical Fenton system [29]. The ferric ion is a strong reduction catalyst; it is reduced in electrical chemical reactions.

3.3. Copper Electrodeposition from Real Leaching Solutions

3.3.1. Copper and Iron Recovery

In this section, the electrodeposition of copper from dilute real leaching solutions that include various impurities (Table 1) was studied. According to Table 1, although the chemical composition of the solutions is similar, there are some differences in heavy metal concentrations (such as Fe, Al), pH, and electrical conductivity.

Figures 9 and 10 show the effect of the cathode potential on the copper recovery and iron removal from the three real leaching solutions. Similar to the results obtained for the synthesized solutions, increasing the cathode potential had a positive effect on the copper recovery.

Higher electrical conductivity of the R-S3 solution (18 mS.cm^{-1}) resulted in higher copper recovery. Similarly, at all cathode potentials, the iron recovery was higher for the R-S3 solution.

Table 4 shows the comparison of the cell performances for the three real leaching solutions and the synthesized solution. According to the results, the value of the energy consumption for the synthetized solution was much lowered (3.03 KWh.kg^{-1}) compared to the values for the real leaching solutions (31-47 KWh.kg^{-1})

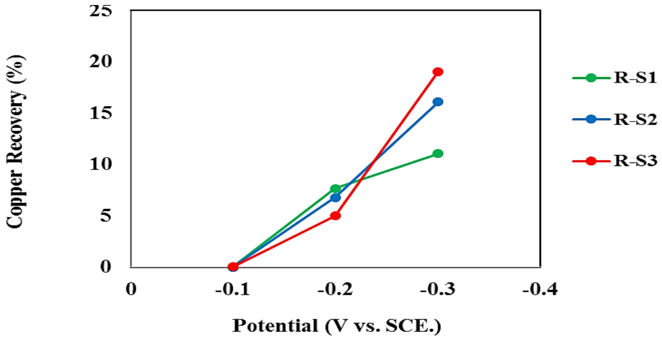

Figure 9. The effect of the cathode potential on the copper electrodeposition from real leaching solutions (T = 26° C ± 1).

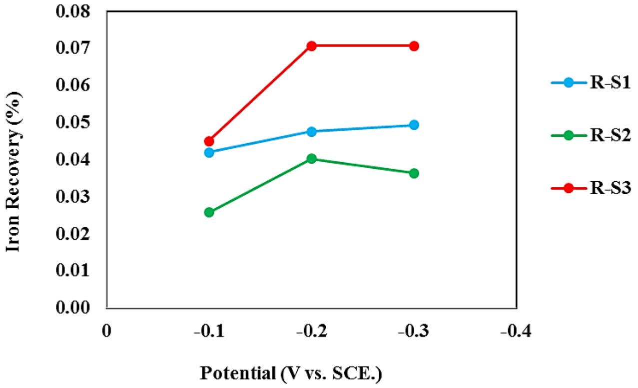

Figure 10. The effect of the cathode potential on the iron electrodeposition from real leaching solutions (T = 26° C ± 1).

Table 4. Cell performance measurements for real leaching solutions (Table 1) and synthesized solution ([Cu (II)] =1000 mg.L^{-1}, [Fe (II)] = 1000 mg.L^{-1}, potential of -0.1 V vs. SCE, T = 26° C ± 1, pH = 2).

Solution type	Time (S)	Average cell voltage (V)	Copper recovery (%)	Cathodic current efficiency (%)	Specific energy consumption (KWh.kg^{-1})
Simulated	7200	2.35	2.830	65.36	3.03
R-S1	7200	1.70	0.031	4.53	31.67
R-S2	7200	1.63	0.027	3.43	40.12
R-S3	7200	2.08	0.034	3.75	46.68

These impurities at certain levels can affect the current efficiency, structure, and morphology of the deposits in the electrowinning process [30]. The presence of Fe (III) in the electrolyte solution decreases the current efficiency which can be attributed to the side reactions involving the reduction of Fe (III) to Fe (II) at the cathode and its generation at the anode. Also, Ferric iron oxidizes copper at the cathode [31]. Furthermore, the addition of Fe (III) adversely influenced the morphology of the copper deposit presumably due to the etching effect of Fe (III) on the deposit [30]. The chemical analysis in Table 1 only shows the total iron concentrations for the real solutions and the portion of Fe (II) and Fe (III) is not clear. So that exact evaluation of the effect of iron is not possible.

The real solutions contain about 3 mg.L^{-1} of Co (II). The cobalt lowers the overpotential of the evolution of oxygen and, hence, the potential of the cell (i.e. reduced energy consumption) [30]. Manganese in the solution can become problematic when it deposits on the surface of the anode as an oxide or oxy-hydroxide, reducing the life of the anode by as much as 18% [32]. The manganese species create a passivation layer on the surface, reducing the effective anode area and increasing the current density on the exposed areas [32]. From Table 1, the R-S3 solution contained less Manganese (144 mg.L^{-1}) compared to two other cases.

An influence of zinc on copper deposit morphology has been detected, although co-deposition of this metal with copper is not possible, due to the very different reduction potentials of Zn (II) and Cu (II) ions [33]. Again, the R-S3 solution contains the less value of Zn (II) (about 17 mg.L^{-1}).

The analysis of the cathode obtained from the real leaching solution (R-S3) showed that co-deposition of Al, Ca, Fe, Mg, Mn, Pb, and Sr happened and the values were calculated as 0.053%, 0.357%, 0.049%, 0.048%, 0.031%, 0.001% and, 3.647%, respectively.

Comparison of the results obtained from the synthesized and real industrial solutions show that copper electrowinning largely depends upon the physicochemical properties of the electrolytes since these properties of the electrolytes affect the energy consumption in the electrochemical cell as shown in Table 4. Hence, the electrowinning operations should be carried out under conditions of high electrical conductivity and high mass transfer conditions to minimize power consumption.

4. Investigation of Diffusion Coefficient for Copper Species in Different Solutions

The movement of charged or neutral species that allows the flow of electricity through an electrolyte solution in an electrochemical cell is referred to as a mass transport process. Migration, diffusion, and convection are the three possible mass transport processes accompanying an electrode reaction. One of the influential parameters on the cementation process is the diffusion coefficient [34]. The purpose of this section is to study the effect of copper, iron, and other metal impurities on the diffusion coefficient for copper species and copper cementation. The recent trends have been directed towards the operation of the electrowinning processes at increased current density. However, this is limited by the limiting current density, i_L, expressed as [35]:

$$i_L = \frac{nFDC_b}{\delta} \tag{10}$$

The i_L value can be increased if the mass transfer conditions in the electrowinning cell can be improved according to [35]:

$$K = \frac{i_L}{n\,F\,C_b} \tag{11}$$

The limiting current density, i_L, is affected by the solution properties, such as viscosity and density, by inhibiting the diffusion of copper ions. This is shown by the following equation [35]:

$$i_L = \frac{k^{\frac{2}{3}} T^{2/3} V_{\infty}^{m} C_b}{(6\pi\gamma_i)^{2/3} k_g \eta^{2/3} (\eta/\rho)^{n}} \tag{12}$$

It has also been shown that the $\eta^{2/3}$ in the above equation contributes more than the term $(\eta/\rho)^n$ to inhibiting diffusion. This indicates that viscosity plays an important role in impeding the diffusion of a species. Therefore, another reason for reducing copper deposition and increasing energy consumption in real solutions could be related to this issue.

The most helpful equation in chronoamperometry is the Cottrell equation, which describes the observed current (planar electrode) at any time following a large forward potential step in a reversible redox reaction (or too large overpotential) as a function of $t^{-1/2}$ according to equation (13):

$$i_t = \frac{nFAC_0D_0^{1/2}}{\pi^{1/2}t^{1/2}} \tag{13}$$

where i_t = diffusion current in time t (A), n = stoichiometric number of electrons involved in the reaction; F = Faraday's constant (96,485 C/equivalent), A = electrode surface area (cm^2), C_0 = concentration of electroactive species (mol/cm^3), and D_0 = diffusion constant for electroactive species (cm^2/s). In practice, the Cottrell equation simplifies to $i_t = k.t^{-1/2}$, where k is a collection of constants for a given system (n, F, A, C_0, D_0). On the one hand, this equation shows the dependence of the current intensity at any moment on the concentration of the chemical compound in the solution, and on the other hand, it shows the decrement of the current in terms of the inverse square root of time ($t^{-1/2}$) [36].

Based on the above equation (13), to investigate the effect of impurities on the diffusion coefficient of copper species in the electrolyte solution, chronoamperometry diagrams were used which were obtained from the laboratory experiments. The solver tool in Microsoft Excel was applied, and by exerting the Cottrell equation (Eq. 13), the error sum of squares (ESS) was minimized. By minimizing the ESS, the value of the diffusion coefficient was determined for the different solutions, including; pure, synthesized, and real solutions.

4.1. The Effect of Iron, Copper, and Metallic Impurities Concentrations on Diffusion Coefficient for Copper Species

The physicochemical properties, such as viscosity, density, and conductivity, of copper electrolyte containing ferrous ions in the range of 0-5000 mg.L^{-1} could be affected on i_L. Both the viscosity and density increase with the increase in ferrous ions in the electrolyte. The impact of ferrous ions on the diffusion coefficient, D, is given in Table 5. The D values decreased with the increase of Fe^{2+} ions concentration up to 5000 mg.L^{-1}. Despite the decrease in the diffusion coefficient, the copper recovery has increased, which could be related to the decrease in internal resistance, increase in electrical current, and therefore enhancement of precipitation rate.

The study of basic kinetic information in high ionic strength electrolytes is a challenging field due to the interactions between ionic species. This can cause significant deviations from the relationship derived for dilute electrolytes. At infinite dilution, the Stokes-Einstein equation explains the inverse relationship between the diffusion coefficient and absolute viscosity as shown in equation (14):

$$D = \frac{RT}{6\pi r \eta N} \tag{14}$$

Where R is the gas constant, T is the temperature in Kelvin, r is the radius of the ionic species, η is the absolute viscosity, and N is Avogadro's number. D is the diffusion coefficient that demonstrates a strong correlation concerning T/η [26].

The effect of iron and other metallic impurities ions on the diffusion coefficient in real solutions is shown in Table 6. Comparison of the results of Table 5 with Table 6 shows the decrement of the diffusion coefficient in real solutions compared to the synthesized solutions, especially in R-S2 solution, (including; total metal content 4650 mg.L^{-1}), which is about 10 times less. It could be related to the viscosity, variety of impurities, and their different ionic radii, which on diffusion coefficient constant is effective and impedes the penetration of copper ions to the proximity to the electrode surface.

Table 5. The effect of Fe^{2+} ions on the diffusion coefficient.

Cu^{2+} (mg/l)	Fe^{2+} (mg/l)	Copper recovery (%)	Diffusion coefficient (D) ($cm^2.s^{-1}$)
1000	0	2.64	$2.27*10^{-4}$
1000	2000	3.65	$8.87*10^{-8}$
1000	5000	5.09	$5.80*10^{-8}$

Table 6. The effect of iron and other metallic impurities ions on the diffusion coefficient.

Solution code	Cu^{2+} (mg/l)	Fe^{2+} (mg/l)	Total metal content (mg/l)	Copper recovery (%)	Diffusion coefficient (D) (cm^2/s)
R-S1	1109	1190	4063	0.031	$2.90*10^{-8}$
R-S2	1114	1550	4650	0.027	$9.40*10^{-9}$
R-S3	1022	1104	3822	0.034	$2.80*10^{-8}$

The obtained results from pure copper solutions show which amount of diffusion coefficients are higher compared to impure and real solutions. As well, increasing the copper concentration from 1000 to 5000 mg.L^{-1} decreased the diffusivity of copper ions. moreover, in pure solutions, the copper recovery is more than other solutions which could be related to increasing the electrical conductivity of the solution and the diffusion coefficient. Also, it is possible to determine the diffusion coefficient by plotting i_t vs. $t^{-1/2}$ and ($i_t.t^{1/2}$) vs. Cu^{2+} concentration in a straight line with a slope of $nFAC_0\pi^{-1/2}D^{1/2}$ and D as seen in Figures 12 and 13, respectively.

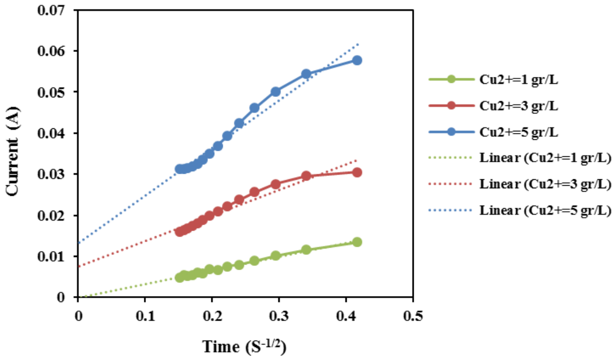

Figure 12. Plots of i vs. $t^{-1/2}$ related to chronoamprograms obtained in different Cu^{2+} concentrations (no agitation, ambient atmosphere).

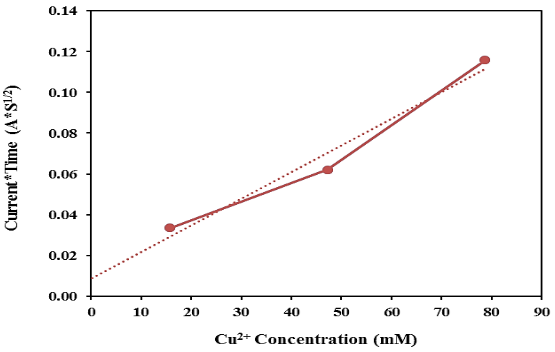

Figure 13. Plot of i_t. $t^{1/2}$ vs. different Cu^{2+} concentrations.

The effect of Cu^{2+} concentration on the value of diffusion coefficient ($D_{Cu}{}^{2+}$) is illustrated in Table 7.

Table 7. The effect of Cu^{2+} concentration on the diffusion coefficient.

Cu^{2+} (mg/l)	Fe^{2+} (mg/l)	Copper recovery (%)	Diffusion coefficient (D) (cm^2/s)
1000	0	2.64	$2.27*10^{-4}$
3000	0	8.43	$7.47*10^{-6}$
5000	0	9.37	$5.39*10^{-8}$

5. Conclusion

Recovery of copper from dilute solutions is a challenging issue both from environmental but also economic points of view. Dilute leaching solutions from mining operations, such as heap leaching, contain low concentrations of copper and various heavy metals as impurities. In this paper, the electrodeposition of copper from synthesized and real dilute sulfuric acid solutions was investigated. Effects of copper and iron concentrations and applied potential were studied. In pure copper solution, increasing the Cu^{2+} concentration from 1000 to 5000 mg.L^{-1} increased the copper recovery from about 30-300% depending on the cathode potential and decreased the energy consumption by about 30%. Also, with increasing the acid concentration from 15 to 50 g.L^{-1} a 25% increase in copper recovery and a 30% decrease in energy consumption were observed. The addition of Fe^{2+} to the solution improved the ionic conductivity and so that the copper recovery. The specified energy consumption for the real acidic leaching solutions increased to 31-47 KWh.kg^{-1}. The diffusion coefficients for several synthesized and real copper electrowinning electrolytes were determined. Moreover, the maximum value of the diffusion coefficient was obtained $2.27*10^{-4}$ cm^2.s^{-1} for the pure copper solution at a concentration of 1000 mg.L^{-1} Cu^{2+}.

Abbreviation

PLS = pregnant leach solution
SCE = saturated calomel electrode
SEC = specific energy consumption
CA = chronoamperometry
ESS = error sum of squares
ORP = oxidation-reduction potential
CE = current efficiency
CV = cyclic voltammetry
RCE = rotating cylinder electrode

Symbols

C_b = concentration of copper in the bulk electrolyte, mol/m^3

D = diffusion coefficient of the electrolyte, m^2/s

D_0 = diffusion constant for electroactive species, cm^2/s

F = Faraday's constant

i_L = limiting current density, A/m^2

K = mass transfer coefficient, mm/s

k = Boltzmann constant

k_g = constant for a given electrode geometry

m, p = constants

n = number of electrons taking part in the reaction

r_i & r = radius of the diffusion ionic species

V_∞ = velocity constant of the electrolyte parallel to the electrode surface at a distance greater compared to diffusion layer thickness

R = gas constant

T = temperature in Kelvin

N = Avogadro's number

Greek

η_L = absolute viscosity of the solution, kg/m.s

ρ = density of the solution, kg/m^3

δ = diffusion layer thickness, m

Acknowledgments

The authors wish to express their gratitude to Yazd University, Iran, for their support.

Funding

This research did not receive any specific grant from funding agencies in public, commercial, or not-for-profit sectors.

REFERENCES

[1] D. Pradhan, S. Pal, L. Sukla, G.R. Chaudhury, T. Das, Bioleaching of low-grade copper ore using indigenous microorganisms, (2008).

[2] A.B. Vakylabad, M. Schaffie, A. Naseri, M. Ranjbar, Z. Manafi, A procedure for processing of pregnant leach solution (PLS) produced from a chalcopyrite-ore bio-heap: CuO Nano-powder fabrication, Hydrometallurgy 163 (2016) 24-32.

[3] M. Gorgievski, D. Božić, V. Stanković, G. Bogdanović, Copper electrowinning from acid mine drainage: a case study from the closed mine "Cerovo", Journal of hazardous materials 170(2-3) (2009) 716-721.

[4] H.I. Maarof, W.M.A.W. Daud, M.K. Aroua, Recent trends in removal and recovery of heavy metals from wastewater by electrochemical technologies, Reviews in Chemical Engineering 33(4) (2017) 359-386.

[5] G. Issabayeva, M.K. Aroua, N.M. Sulaiman, Electrodeposition of copper and lead on palm shell activated carbon in a flow-through electrolytic cell, Desalination 194(1-3) (2006) 192-201.

[6] S.A. Mirbagheri, S.N. Hosseini, Pilot plant investigation on petrochemical wastewater treatment for the removal of copper and chromium with the objective of reuse, Desalination 171(1) (2005) 85-93.

[7] A. El Samrani, B. Lartiges, F. Villiéras, Chemical coagulation of combined sewer overflow: heavy metal removal and treatment optimization, Water research 42(4-5) (2008) 951-960.

[8] L. Monser, N. Adhoum, Modified activated carbon for the removal of copper, zinc, chromium, and cyanide from wastewater, Separation, and purification technology 26(2-3) (2002) 137-146.

[9] M. Mohsen-Nia, P. Montazeri, H. Modarress, Removal of Cu2+ and Ni2+ from wastewater with a chelating agent and reverse osmosis processes, Desalination 217(1-3) (2007) 276-281.

[10] N. Touabi, S. Martinez, M. Bounoughaz, Optimization of electrochemical copper recovery process: effect of the rotation speed in chloride medium of pH= 3, Int. J. Electrochem. Sci 10 (2015) 7227-7240.

[11] P. Rodenas Motos, A. ter Heijne, R. van der Weijden, M. Saakes, C.J. Buisman, T.H. Sleutels, High rate copper and energy recovery in microbial fuel cells, Frontiers in microbiology 6 (2015) 527.

[12] Z. Wang, B. Lim, H. Lu, J. Fan, C. Choi, Cathodic reduction of Cu2+ and electric power generation using a microbial fuel cell, B Korean Chem Soc 31 (2010) 2025-2030.

[13] X. Guo, H. Qin, Q. Tian, D. Li, Recovery of metals from waste printed circuit boards by selective leaching combined with cyclone electrowinning process, Journal of hazardous materials 384 (2020) 121355.

[14] J.A. Barragan, C. Ponce de León, J.R. Alemán Castro, A. Peregrina-Lucano, F. Gómez-Zamudio, E.R. Larios-Durán, Copper and antimony recovery from electronic waste by hydrometallurgical and electrochemical techniques, ACS omega 5(21) (2020) 12355-12363.

[15] P.-M. Hannula, M.K. Khalid, S. Kinnunen, P. Halli, D. Janas, K. Yliniemi, M. Lundström, Recovery of copper from low concentration wastewaters by electrowinning, International Mine Water Association Congress–"Mine Water & Circular Economy–A Green Congress, 2017.

[16] M. Moats, M. Free, A bright future for copper electrowinning, Jom 59(10) (2007) 34-36.

[17] M.E. Schlesinger, K.C. Sole, W.G. Davenport, Extractive metallurgy of copper, Elsevier2011.

[18] S. Das, P.G. Krishna, Effect of Fe (III) during copper electrowinning at higher current density, International journal of mineral processing 46(1-2) (1996) 91-105.

[19] D. Dew, C. Phillips, The effect of Fe (II) and Fe (III) on the efficiency of copper electrowinning from dilute acid Cu (II) sulphate solutions with the Chemelec cell. Part II. The efficiency of copper electrowinning from dilute liquors, Hydrometallurgy 14(3) (1985) 351-367.

[20] A. Monhemius, P. Costa, Interactions of variables in the fluidised-bed electrowinning of copper, Hydrometallurgy 1(2) (1975) 183-203.

[21] P.-M. Hannula, M.K. Khalid, D. Janas, K. Yliniemi, M. Lundström, Energy-efficient copper electrowinning and direct deposition on carbon nanotube film from industrial wastewaters, Journal of Cleaner Production 207 (2019) 1033-1039.

[22] A. Bard, Electrochemical Methods, Fundamentals, and applications 290 (1980).

[23] E. Shahrivar, M. Karamoozian, M. Gharabaghi, Modeling and optimization of oxide copper cementation kinetics, SN Applied Sciences 2(3) (2020) 1-13.

[24] M.S. Rana, M.A. Rahman, A.S. Alam, A Cyclic Voltammetric Studies of Complexation of Copper (II) with Thymine Using Glassy Carbon Electrode in Aqueous Medium, Pakistan Journal of Analytical & Environmental Chemistry 15(2) (2014) 7.

[25] A.A.-M.A. Owais, Packed bed electrolysis for production of electrolytic copper powder from electronic scrap, Shaker2003.

[26] M.S. Moats, J.B. Hiskey, D.W. Collins, The effect of copper, acid, and temperature on the diffusion coefficient of cupric ions in simulated electrorefining electrolytes, Hydrometallurgy 56(3) (2000) 255-268.

[27] A. Izadi, A. Mohebbi, M. Amiri, N. Izadi, Removal of iron ions from industrial copper raffinate and electrowinning electrolyte solutions by chemical precipitation and ion exchange, Minerals Engineering 113 (2017) 23-35.

[28] A. Cooke, J. Chilton, D. Fray, Mass-transfer kinetics of the ferrous-ferric electrode process in copper sulphate electrowinning electrolytes, Institution of Mining and Metallurgy Transactions. Section C. Mineral Processing and Extractive Metallurgy 98 (1990).

[29] S. Karthikeyan, A. Titus, A. Gnanamani, A. Mandal, G. Sekaran, Treatment of textile wastewater by homogeneous and heterogeneous Fenton oxidation processes, Desalination 281 (2011) 438-445.

[30] F. Erdemir, The Influence of Impurity Ions on The Electrowinning of Copper from Waste PCBs Leaching Solutions.

[31] B. McKevitt, D. Dreisinger, A comparison of various ion exchange resins for the removal of ferric ions from copper electrowinning electrolyte solutions part I: Electrolytes containing no other impurities, Hydrometallurgy 98(1-2) (2009) 116-121.

[32] P. Laforest, Understanding Impurities in copper electrometallurgy, (2015).

[33] L. Muresan, A. Nicoara, S. Varvara, G. Maurin, Influence of Zn2+ ions on copper electrowinning from sulfate electrolytes, Journal of applied electrochemistry 29(6) (1999) 723-731.

[34] J. Agar, Diffusion and convection at electrodes, Discussions of the Faraday Society 1 (1947) 26-37.

[35] T. Subbaiah, S. Das, Effect of some common impurities on mass transfer coefficient and deposit quality during copper electrowinning, Hydrometallurgy 36(3) (1994) 271-283.

[36] A. Kamat, A. Huth, O. Klein, S. Scholl, Chronoamperometric investigations of the electrode-electrolyte interface of a commercial high-temperature PEM fuel cell, Fuel Cells 10(6) (2010) 983-992